FRAM: Frobenius-Regularized Assignment Matching with Mixed-Precision Computing

Binrui Shen[1,2], Yuan Liang[3], and Shengxin Zhu*[4,5]

[1]School of Mathematical Sciences, Laboratory of Mathematics and Complex Systems, MOE, Beijing Normal University, Beijing 100875, P.R. China
[2]Faculty of Arts and Sciences, Beijing Normal University, Zhuhai 519087, P.R. China
[3]School of Mathematical Sciences, Beijing Normal University, Beijing 100875, P.R. China
[4]Research Centers for Mathematics, Advanced Institute of Natural Science, Beijing Normal University, Zhuhai 519087, P.R. China
[5]Guangdong Provincial Key Laboratory of Interdisciplinary Research and Application for Data Science, BNU-HKBU United International College, Zhuhai 519087, P.R. China
binrui.shen@bnu.edu.cn, l.y@mail.bnu.edu.cn, Shengxin.Zhu@bnu.edu.cn

Abstract

Graph matching, usually cast as a discrete Quadratic Assignment Problem (QAP), aims to identify correspondences between nodes in two graphs. Since QAP is NP-hard, many methods its discrete constraints by projecting the discrete feasible set onto its convex hull and solving the resulting continuous problem. However, these relaxations inevitably enlarge the feasible set and introduce two errors: sensitivity to numerical scales and geometric misalignment between the relaxed and original feasible domains. To address these issues, we propose a novel relaxation framework to reformulate the projection step as a Frobenius-Regularized Linear Assignment (FRA) problem. This formulation incorporates a tunable regularization term to curb the inflation of the feasible region and ensure numerical scale invariance. To solve the FRA efficiently, we introduce a scaling algorithm for doubly stochastic normalization. Leveraging its favorable computational properties, we design a theoretically grounded, accelerated mixed-precision algorithm. Building on these components, we propose Frobenius-Regularized Assignment Matching (FRAM), which approximates the QAP solution through a sequence of FRA problems. Extensive CPU experiments show that FRAM consistently outperforms all baselines. On GPUs, with mixed precision, FRAM achieves up to a 370× speedup over its FP64 CPU implementation without sacrificing accuracy.

1 Introduction

Graph matching aims to find correspondences between graphs that share potential relationships. It can be used in various fields of intelligent information processing, e.g., image similarity detection [33], graph similarity computation [19, 20], knowledge graph alignment [40], autonomous driving [36], vision-language model alignment [30], point cloud registration [10], deep neural network fusion [25], multi-object tracking [14], and COVID-19 disease mechanism study [13]. However, graph matching is an NP-hard discrete optimization problem [32] and computationally prohibitive for large-scale instances.

To scale up the graph matching problem, many relaxation methods were proposed [2, 5, 12, 21, 27, 34]. These methods relax the discrete problem to a continuous domain and then project the

*Communication author

39th Conference on Neural Information Processing Systems (NeurIPS 2025).

continuous solution back to the original discrete domain. The doubly stochastic projection is a typical representative and frequently used recently [27, 43]. This projection maps the gradient matrix onto the convex hull of the original domain. However, such relaxations inevitably enlarge the feasible region and result in two sources of errors: (1) geometric misalignment between the relaxed and original domains, which undermines the quality of the recovered integer solution; and (2) the loss of numerical scale invariance due to the projections in the nonconvex setting. Such limitations motivate our current research.

Our contributions include

1. **Theoretical results**: We extend the doubly stochastic projection to the FRA by introducing a tunable regularization parameter that controls relaxation-induced distortion. We provide a thorough analysis of how the regularization parameter affects performance, and address the numerical scale sensitivity through an integrated normalization mechanism.
2. **Algorithm**: we propose FRAM, a graph matching algorithm, that solves the QAP approximately by iteratively solving a sequence of FRA problems. Each FRA problem can be solved efficiently by our proposed Scaling Doubly Stochastic Normalization (SDSN). Empirical evaluations show that FRAM achieves superior performance compared to state-of-the-art baselines.
3. **Computing acceleration**: We develop a theoretically grounded mixed-precision implementation of FRAM. Compared to CPU-based double-precision computation, it achieves up to a 370× speedup on an NVIDIA RTX 4080 SUPER GPU across some benchmark problems, with at most a 0.2% drop in accuracy. To the best of our knowledge, this is the first graph matching algorithm built upon a theoretically grounded mixed-precision design.

2 Related Works

Related graph matching algorithms. We categorize related graph matching algorithms into three representative classes. (1) Methods based on doubly stochastic optimization: these works employ continuous relaxations. Graduated Assignment (GA) [12] pioneers this approach via a sequence of linear approximations. Adaptive softassign [34] improves GA by automatically tuning an entropic parameter. IPFP [22] projects gradients onto permutations, while DSN [43] finds the nearest doubly stochastic matrix. DSN is adopted by [27] for gradient projection. (2) Spectral-based methods: these approaches leverage spectral properties. Typical methods [21, 35] recover assignments from the leading eigenvector. The method in [5] adds affine constraints to improve accuracy while maintaining speed. Recent research [16] connects eigenvectors to multiscale structural features. (3) Methods based on optimal transport: these techniques formulate graph matching as an optimal transport problem. GWL [39] measures graph distance via Gromov-Wasserstein discrepancy, while S-GWL [38], a scalable variant, applies a divide-and-conquer strategy to enhance efficiency. For a comprehensive survey, we refer readers to [8, 41].

Mixed-precision computing is a sophisticated technique for accelerating computationally intensive applications. It has been successfully applied to solving linear systems [4, 15] and large-scale AI models such as DeepSeek-V3 [24]. However, little attention has been paid to its use in the graph matching context, partly due to a lack of theoretical understanding. The main challenges in mixed-precision computing stem from (1) the limited range of lower-precision formats, which increases the risk of overflow or underflow, and (2) rounding errors introduced by lower-precision operations, which may lead to error propagation [28]. See [17] for more details on mixed-precision algorithms. This paper provides theoretical guarantees for a mixed-precision graph matching algorithm, achieving both numerical stability and computational speedups.

3 Preliminaries

An *undirected attributed graph* $G = \{V, E, A, F\}$ consists of a finite set of nodes $V = \{1, \ldots, n\}$ and a finite set of edges $E \subset V \times V$. The matrix A is a nonnegative symmetric *edge-attribute matrix* whose element A_{ij} specifies the attribute of the edge between nodes i and j. The i-th row of the feature matrix F represents the attribute vector of node i.

Matching matrix. Given two attributed graphs $G = V, E, A, F$ and $\tilde{G} = \tilde{V}, \tilde{E}, \tilde{A}, \tilde{F}$, we first assume that the two graphs have the same number of vertices, i.e., $n = \tilde{n}$, for simplicity. A matching matrix $M \in \mathbb{R}^{n\times n}$ encodes the correspondence between nodes: $M_{i\tilde{i}} = 1$ if node i in G matches node $\tilde{i}$ in $\widetilde{G}$, and $M_{i\tilde{i}} = 0$ otherwise. Under the one-to-one constraint, a matching matrix is a permutation matrix. The set of permutation matrices is denoted as $\Pi_{n\times n} = \{M : M\mathbf{1} = \mathbf{1}, M^T\mathbf{1} = \mathbf{1}, M \in \{0, 1\}^{n\times n}\}$, where $\mathbf{1}$ represents vectors with all ones.

Continuous relaxation. The graph matching problem is typically formulated as a QAP that is NP-hard [11]. A common strategy to handle such discrete problems is relaxation. It first finds a solution on $\mathcal{D}_{n\times n} := \{N : N\mathbf{1} = \mathbf{1}, N^T\mathbf{1} = \mathbf{1}, N \geq 0\}$ which is the convex hull of the original domain. The relaxed problem is then formulated as

$$N^* = \arg\max_{N\in\mathcal{D}_{n\times n}} \Phi(N), \quad \Phi(N) = \tfrac{1}{2}\underbrace{\mathrm{tr}(N^T A N \widetilde{A})}_{\text{Edges' similarites}} + \lambda \underbrace{\mathrm{tr}(N^T K)}_{\text{Nodes' similarites}}, \tag{1}$$

where λ is a parameter, $K = F\tilde{F}^T$, and $\mathrm{tr}(\cdot)$ represents the trace operator. And then N^* is transformed back to the original discrete domain $\Pi_{n\times n}$ by solving a *linear assignment problem*:

$$M = \arg\min_{P\in\Pi_{n\times n}} \|P - N^*\|_F. \tag{2}$$

The matrix M is the final solution. Although relaxation allows the use of continuous optimization, the problem (1) is non-convex and thus remains NP-hard [31]. Hence, existing algorithms typically aim to obtain high-quality approximate solutions within acceptable time. Further discussions on convex relaxations and their constructions can be found in [1, 6, 9].

The projected fixed-point method. Many existing methods [5, 12, 22, 27, 34] adopt a similar iterative framework to efficiently approximate the objective in (1):

$$\begin{aligned} N^{(t+1)} &= (1-\alpha)N^{(t)} + \alpha D^{(t)}, \\ D^{(t)} &= \mathcal{P}(\nabla\Phi(N^{(t)})) = \mathcal{P}(AN^{(t)}\tilde{A} + \lambda K), \end{aligned} \tag{3}$$

where α is a step-size parameter and $\mathcal{P}(\cdot)$ is an operator which maps the gradient matrix onto a certain set. When the solution domain is relaxed to the convex hull of the original domain (i.e., the set of doubly stochastic matrices), a natural choice for $\mathcal{P}(\cdot)$ is the doubly stochastic projection [27, 43]. It finds the closest doubly stochastic matrix to the gradient matrix $\nabla\Phi(N^{(t)})$ in terms of the Frobenius norm:

$$\mathcal{P}_{\mathcal{D}}(X) = \arg\min_{D\in\mathcal{D}_{n\times n}} \|D - X\|_F. \tag{4}$$

The resulting algorithm is the Doubly Stochastic Projected Fixed-Point method (DSPFP) [27].

4 Projection to Assignment

We first propose a regularized linear assignment formulation by examining the numerical sensitivity of the doubly stochastic projection, and then analyze how the regularization parameter affects performance.

4.1 Doubly stochastic projection to assignment

It can be observed that the solution to the quadratic assignment problem (1) also maximizes $w\Phi(N)$, where w is a positive scaling constant. This reflects the numerical scale-invariant property of the objective. However, the doubly stochastic projection $\mathcal{P}_{\mathcal{D}}(\cdot)$ fails to preserve this property:

$$\mathcal{P}_{\mathcal{D}}(X) \neq \mathcal{P}_{\mathcal{D}}(wX), \qquad \text{for } X \in \mathbb{R}_+^{n\times n}. \tag{5}$$

Since the objective function is non-convex, this sensitivity can cause the projection-based algorithm to converge to different points under different scalings.

To elaborate the sensitivity, consider:

$$\mathcal{P}_{\mathcal{D}}(wX) = \arg\min_{D\in\mathcal{D}_{n\times n}} \|D - wX\|_F = \arg\min_{D\in\mathcal{D}_{n\times n}} \|D - wX\|_F^2. \tag{6}$$

By expanding the quadratic norm, we have

$$\|D - wX\|_F^2 = \langle D, D\rangle - 2\langle D, wX\rangle + \langle wX, wX\rangle, \tag{7}$$

where $\langle \cdot, \cdot \rangle$ represents the Frobenius inner product. Since $\langle wX, wX\rangle$ is independent of D, it does not affect the optimization. Thus,

$$\mathcal{P}_{\mathcal{D}}(wX) = \arg \min_{D \in \mathcal{D}_{n\times n}} \langle D, D\rangle - 2w\langle D, X\rangle. \tag{8}$$

As a result, the problem reduces to

$$\mathcal{P}_{\mathcal{D}}(wX) = \arg \max_{D \in \mathcal{D}_{n\times n}} \langle D, X\rangle - \frac{1}{2w}\langle D, D\rangle. \tag{9}$$

$\langle D, X\rangle$ represents an assignment score.

By referring back to the update formula (3), X corresponds to the gradient matrix $\nabla\Phi(N^{(t)})$:

$$\mathcal{P}_{\mathcal{D}}(w\nabla\Phi(N^{(t)})) = \arg \max_{D \in \mathcal{D}_{n\times n}} \langle D, \nabla\Phi(N^{(t)})\rangle - \frac{1}{2w}\langle D, D\rangle. \tag{10}$$

$$= \arg \max_{D \in \mathcal{D}_{n\times n}} \langle D, AN^{(t)}\tilde{A} + \lambda K\rangle - \frac{1}{2w}\langle D, D\rangle \tag{11}$$

$$= \arg \max_{D \in \mathcal{D}_{n\times n}} \operatorname{tr}(D^T AN^{(t)}\widetilde{A}) + \lambda \operatorname{tr}(D^T K) - \frac{1}{2w}\langle D, D\rangle \tag{12}$$

Intuitively, higher assignment scores in (12) lead to larger objective values (1) during the iterative process. As w increases, the projection process emphasizes optimizing the objective assignment score (1). Conversely, when w decreases, the significance of the objective assignment score diminishes. This finding characterizes how the scaling constant w affects the optimization process.

Motivated by the above observation, we propose converting the uncontrollable scaling constant w of the problem into a controllable modeling parameter θ, as follows. Specifically, we extend the doubly stochastic projection to a Frobenius-regularized linear assignment problem by introducing a modeling parameter θ, leading to the following formulation.

Theorem 1. *The solution to the scaled doubly stochastic projection problem*

$$D_X^\theta = \arg \min_{D \in \mathcal{D}_{n\times n}} \|D - \tfrac{\theta}{2}X\|_F^2 \tag{13}$$

is equivalent to the solution of a Frobenius-regularized linear assignment problem:

$$D_X^\theta = \arg \max_{D \in \mathcal{D}_{n\times n}} \Gamma^\theta(X), \quad \Gamma^\theta(X) = \langle D, X\rangle - \tfrac{1}{\theta}\langle D, D\rangle. \tag{14}$$

Furthermore, the flexibility of this formulation allows us to normalize the input matrix X by dividing it by $\max(X)$, thereby eliminating the influence of the scaling constant w. Consequently, the weighting of the assignment term during optimization is entirely controlled by θ.

4.2 Convergence to optimal assignment

To investigate the properties of FRA, we analyze the limiting behavior of D_X^θ as θ approaches infinity and 0.

Theorem 2. *Let $X \in \mathbb{R}_+^{n\times n}$ and $\mathcal{F}$ be the convex hull of the optimal permutation matrices for the linear assignment problem with X. As $\theta \to \infty$, the matrix D_X^θ converges to a unique matrix $D^* \in \mathcal{F}$, where D^* is the unique solution to* $\min_{D\in\mathcal{F}} \frac{1}{\theta}\langle D, D\rangle$.

This theorem reveals a key advantage of FRA: unlike standard linear assignment solvers [22] that return an optimal permutation and discard others, D_X^θ approximates a convex combination of all optimal permutations, preserving richer solution information.

Corollary 1. *If there is only one optimal permutation, then D_X^θ converges to the corresponding permutation matrix.*

When D_X^θ corresponds to the unique permutation matrix, our algorithm becomes equivalent to IPFP [22] and the classical Frank–Wolfe algorithm [37]. In contrast, when multiple optimal permutations exist, our matching algorithm can capture a richer set of high-quality matches than these two methods [22, 37]. However, if θ is chosen too small, the resulting matrix D_X^θ may fail to reveal high-quality correspondences, as the following proposition demonstrates.

Proposition 1. *As $\theta \to 0$, the matrix D_X^θ converges to the matrix $\frac{\mathbf{1}\mathbf{1}^T}{n}$.*

4.3 Influence of the parameter

To analyze the impact of the parameter, we quantify the solution quality through a distance metric between D_X^θ and D_X^∞ for a given matrix $X \in \mathbb{R}_+^{n\times n}$. The total assignment score $\langle D^\theta, X\rangle$ scales with the problem size. To enable scale-independent error analysis, we define a *normalized assignment error* to quantify the performance gap:

$$\epsilon_X^\theta = \frac{1}{n}\left(\langle D_X^\infty, X\rangle - \langle D_X^\theta, X\rangle\right) \tag{15}$$

This normalization effectively decouples the approximation error from the problem scale, providing a stable metric to assess the quality of D_X^θ across different numbers of nodes—like how the *Mean Squared Error* (MSE) serves as a scale-independent alternative to the *Sum of Squared Errors*.

Proposition 2. *For a matrix $X \in \mathbb{R}_+^{n\times n}$, the following inequality holds:*

$$\epsilon_X^\theta \le \tfrac{1}{\theta}. \tag{16}$$

This proposition establishes that the performance gap between D_X^θ and D_X^∞ is bounded by $1/\theta$. This theoretical bound guarantees the stability and accuracy of our approximation scheme, ensuring that the solution asymptotically approaches optimal performance as θ becomes sufficiently large.

Figure 1 illustrates how the matrix D_X^θ evolves as θ varies. When θ is small, the matrix entries are nearly uniform. As θ increases, D_X^θ progressively approaches a permutation matrix that lies within the original feasible domain of the QAP. This observation demonstrates that a larger θ effectively suppresses the bias introduced by relaxation. By selecting an appropriate value of θ, the intermediate solution during the matching process remains confined to a relaxed region that stays close to the original feasible domain of graph matching problems.

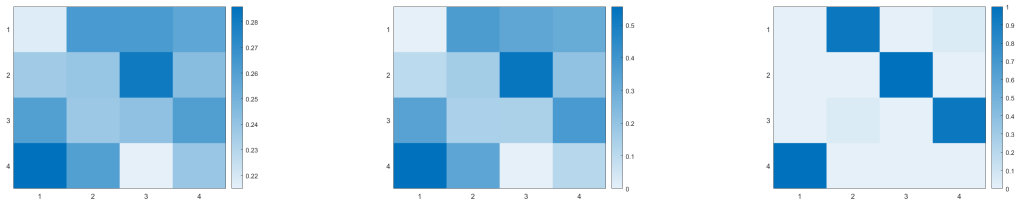

(a) $\theta = 0.1$ (b) $\theta = 1$ (c) $\theta = 10$

Figure 1: Visualization of D_X^θ under different values of θ. The color of each cell represents the matrix entry, with darker shades indicating larger values.

When FRA serves as a component within the graph matching framework (3), increasing θ generally improves the per-iteration matching score by enforcing sharper correspondences. However, an excessively large θ may slightly degrade the final matching performance due to premature convergence. This phenomenon can be interpreted from a probabilistic perspective, where each entry in the doubly stochastic matrix D_X^θ represents the probability of a potential correspondence. A large θ may lead to overconfident assignments at early stages, thereby hindering the exploration of alternative matching possibilities.

5 Scaling Doubly Stochastic Normalization

This section introduces the Scaling Doubly Stochastic Normalization (SDSN) method to efficiently solve the FRA. The method is further adapted to achieve low-precision acceleration, accompanied by theoretical guarantees.

5.1 Doubly stochastic normalization

Due to the equivalence between FRA and the scaling doubly stochastic projection, FRA admits a solution via tailored modifications of standard projection algorithms. Zass and Shashua [43] solved

the doubly stochastic projection (4) by alternately solving two subproblems:

$$\mathcal{P}_1(X) = \arg\min_{Y\mathbf{1}=Y^T\mathbf{1}=\mathbf{1}} \|X-Y\|_F, \quad \mathcal{P}_2(X) = \arg\min_{Y\geq 0} \|X-Y\|_F^2 \tag{17}$$

The von-Neumann successive projection lemma [29] states that $\mathcal{P}_2\mathcal{P}_1\mathcal{P}_2\mathcal{P}_1\ldots\mathcal{P}_2\mathcal{P}_1(X)$ converges to $\mathcal{P}_{\mathcal{D}}(X)$. The derived doubly stochastic normalization (DSN) [43] for $X \in \mathbb{R}_+^{n\times n}$ works as follows.

$$\tilde{X}^{(k)} = \mathcal{P}_1\left(X^{(k-1)}\right), \;\; X^{(k)} = \mathcal{P}_2\left(\tilde{X}^{(k)}\right), \tag{18}$$

$$\mathcal{P}_1(X) = X + \left(\frac{I}{n} + \frac{\mathbf{1}^T X \mathbf{1}}{n^2} I - \frac{\mathbf{X}}{n}\right)\mathbf{1}\mathbf{1}^T - \frac{\mathbf{1}\mathbf{1}^{\mathbf{T}}\mathbf{X}}{n}, \qquad \mathcal{P}_2(X) = \frac{X+|X|}{2}, \tag{19}$$

where I is the $n \times n$ identity matrix. It alternately applies row and column normalization $\mathcal{P}_1$ and non-negativity enforcement $\mathcal{P}_2$ for the doubly stochastic property. Each iteration requires $O(n^2)$ operations. The DSN algorithm converges linearly, meaning that there exists a constant $0 < c < 1$ such that $c = \lim_{k\to\infty} \frac{\|X^{(k+1)}-X^*\|}{\|X^{(k)}-X^*\|}$.

5.2 Convergence criterion

An explicit convergence criterion is notably absent in DSN. Zass and Shashua [43] terminated the iterations once the updated matrix became doubly stochastic. However, this approach is computationally expensive and thus inefficient for large-scale tasks. In contrast, Lu et al. [27] fixed the number of iterations to 30 to improve efficiency, but this heuristic did not guarantee that the output matrix remained doubly stochastic.

We propose a criterion to quantify the deviation between the current matrix and the ideal solution. To ensure dimension-invariant analysis and computational efficiency, we define a **dimensional scaled error** as

$$\gamma(X^{(k)}) = \frac{1}{n}\sum_{i,j} X_{ij}^{(k)} - 1 = \frac{\mathbf{1}^T X^{(k)} \mathbf{1}}{n} - 1. \tag{20}$$

Normalization by n ensures that the metric remains comparable across matrices of different sizes. A detailed derivation of the convergence condition is provided in Appendix B, and the overall process is illustrated in Figure 2.

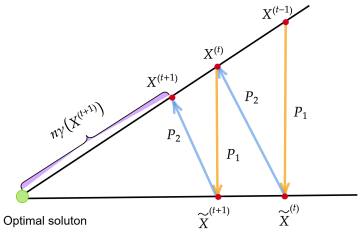

Figure 2: Convergence process of SDSN.

5.3 Number of iterations

The SDSN is summarized in Algorithm 2. We analyze the influence of the parameter θ on the number of SDSN iterations in the following theorem, which shows that the iteration count grows proportionally with the value of θ.

Proposition 3. *For $X \in \mathbb{R}_+^{n\times n}$, the SDSN algorithm requires*

$$\left\lceil \ln\left(\frac{\epsilon}{\theta(\|X\|_F + n)}\right)\frac{1}{\ln(c)} \right\rceil$$

iterations to produce a solution X^* that satisfies $\|X^* - D_X^\theta\|_F < \epsilon$ where D_X^θ is the exact solution and $c \in (0,1)$ is the convergence rate constant of the DSN algorithm.

5.4 Robustness to rounding error

Our method leverages a unique property of SDSN, where the effect of rounding errors diminishes over iterations. This enables theoretically guaranteed low-precision acceleration on modern GPUs. The preservation of accuracy is theoretically guaranteed, ensuring the stability and correctness of the entire process.

Theorem 3. *In the SDSN algorithm, the k-th iterate X_k can be split as $X_k = \hat{X}_k + \Delta X_k$, where ΔX_k represents the rounding error. Then, the projection operator satisfies*

$$\mathcal{P}_1(X_k) = \mathcal{P}_1(\hat{X}_k) + \mathcal{P}_3(\Delta X_k),$$

where $\mathcal{P}_3(\Delta X)$ is the solution to the following minimization problem:

$$\mathcal{P}_3(\Delta X) = \arg\min_{Y} \|\Delta X - Y\|_F^2, \quad \textit{s.t. } Y\mathbf{1} = \mathbf{0},\ Y^\top \mathbf{1} = \mathbf{0}.$$

The subsequent transformations of the error term ΔX_k can be expressed as

$$\mathcal{P}_2\mathcal{P}_3 \cdots \mathcal{P}_2\mathcal{P}_3(\Delta X_k),$$

which asymptotically converges to the zero matrix $\mathbf{0}_{n\times n}$.

This property of SDSN prevents the accumulation of rounding errors arising from both the gradient-matrix computation in (3) and the subsequent SDSN operations that correspond to ΔX_0 and $\{\Delta X_k\}_{k\geq 1}$. Therefore, this property enables efficient low-precision computation with negligible loss of accuracy.

6 Matching Algorithm

We propose the Frobenius-Regularized Assignment Matching (FRAM) algorithm[2], which approximates the QAP via a sequence of FRA problems. Each FRA is efficiently solved by the scalable SDSN solver. The overall procedure of FRAM is summarized in Algorithm 1.

Mixed-precision Design on GPU. The selection of numerical precision for each operation is detailed in inline code annotations. Steps 2-3 perform matrix scaling enabling stable low-precision acceleration in steps 5 and 6. This scaling adjustment is offset by the normalization in SDSN. The subsequent steps are conducted in double precision to compensate for the accuracy degradation. Further implementation details are provided in Appendix D.

Complexity. For $n = \tilde{n}$, steps 2–3 require $O(n^2)$ operations. Step 5 requires $O(n^3)$ operations per iteration, regardless of whether fast or sparse matrix computations are used. Step 6 requires $O(ln^2)$ operations where l denotes the number of iterations in SDSN. Step 10 transforms the doubly stochastic matrix N back to a matching matrix M using the Hungarian method [18], which has a worst-case complexity of $O(n^3)$. In practice, the cost is significantly lower because N is sparse in most cases. In short, this algorithm has time complexity $O(n^3 + ln^2)$ per iteration and space complexity $O(n^2)$.

Algorithm 1 Frobenius-Regularized Assignment Matching (FRAM)

Require: $A, \tilde{A}, K, \lambda, \alpha, \theta, \delta_{th}$
1: Initial $X^{(0)} = \mathbf{0}_{n\times\tilde{n}}$
2: $c = \max(A, \tilde{A}, K)$ ▷ FP64
3: $A = A/\sqrt{c},\ \tilde{A} = \tilde{A}/\sqrt{c},\ K = K/\sqrt{c}$ ▷ FP64
4: **while** $\delta^{(t)} > \delta_{th}$ **do**
5: $X^{(t)} = AN^{(t-1)}\tilde{A} + \lambda K$ ▷ TF32
6: $D^{(t)} = \text{SDSN}(X^{(t)}, \theta)$ ▷ FP32
7: $N^{(t)} = (1-\alpha)N^{(t-1)} + \alpha D^{(t)}$ ▷ FP64
8: $\delta^{(t)} = \|N^{(t)} - N^{(t-1)}\|_F / \|N^{(t)}\|_F$ ▷ FP64
9: **end while**
10: *Discretize N to obtain M* ▷ FP64
11: **return** Matching matrix M

Algorithm 2 Scaling Doubly Stochastic Normalization (SDSN)

Require: Matrix X, θ, γ_{th}
1: $X^{(0)} = \frac{\theta}{2} X / \max(X)$
2: **while** $\gamma^{(k)} > \gamma_{th}$ **do**
3: $\bar{X}^{(k)} = \frac{\mathbf{1}^T X \mathbf{1}}{n^2}$
4: $X_1^{(k)} = \left(\frac{\mathbf{I}}{n} + \bar{X}^{(k)} I - \frac{X^{(k)}}{n}\right)\mathbf{1}\mathbf{1}^T$
5: $\tilde{X}^{(k+1)} = X^{(k)} + X_1^{(k)} - \frac{\mathbf{1}\mathbf{1}^T X^{(k)}}{n}$
6: $X^{(k+1)} = (\tilde{X}^{(k+1)} + |\tilde{X}^{(k+1)}|)/2$
7: $\gamma^{(k)} = n\bar{X}^{(k)} - 1$
8: **end while**
9: **Output:** Doubly stochastic matrix X

[2] https://github.com/BinruiShen/FRAM

7 Experiments

We evaluate the proposed algorithm (FRAM) and our additional contributions from the following perspectives:

- **Q1.** What improvements does FRAM deliver over baselines on attributed graph matching tasks?
- **Q2.** How robust is FRAM on attribute-free graph matching tasks?
- **Q3.** How does the mixed-precision design accelerate FRAM?

In addition, we discuss the regularization parameter in Appendix F.

Setting. For FRAM, we set $\theta = 2$ for attributed graph matching tasks and $\theta = 10$ for unattributed tasks. Following [27], we set the regularization parameter to $\lambda = 1$ in our experiments, since the results are not sensitive to λ. We configure α to 0.95 to align with the parameter settings used in DSPFP [27]. All algorithmic comparison experiments are conducted in Python 3 on a workstation equipped with an Intel Core i7 (2.80 GHz) processor. All numerical computations are performed in double precision (FP64) to ensure numerical stability. Typical algorithms such as ASM and GA involve exponential operations and are sensitive to floating-point precision. For evaluating the mixed-precision design, we utilize a hardware platform equipped with an Intel Core i9-14900 (3.20 GHz) CPU and an NVIDIA RTX 4080 SUPER GPU.

Dataset. We evaluate our algorithm on three types of graph data: graphs with attributes on both edges and nodes, graphs with attributed edges only, and graphs without attributes. The dataset specifications are summarized in Table 1, and the graph construction procedure from images is described in Appendix E.

Dataset	$\lvert V\rvert$	$\lvert E\rvert$	Attributed nodes	Attributed edges	Ground-truth	Dense graphs
Real-world pictures	(700,1000)	(244 650, 499 500)	✓	✓	✗	✓
CMU House	(600,800)	(179 700, 319 600)	✗	✓	✗	✓
Facebook-ego	4 039	88 234	✗	✗	✓	✗

Table 1: Datasets. $|V|$ is the number of nodes and $|E|$ is the number of edges. (,) represents a range.

Criteria. For attributed graph matching tasks, we evaluate the matching error of algorithms by

$$\frac{1}{2}\left\|A - M\widetilde{A}M^T\right\|_F^2 + \left\|F - M\tilde{F}\right\|_F^2. \tag{21}$$

This formulation is mathematically equivalent to the original objective function (1), differing only by an additive constant and a scaling factor. These terms do not affect the optimization process, while the new formulation provides a more intuitive understanding of the problem. For graphs containing only edge attribute matrices, the metric reduces to the first term of (21). For attribute-free graph matching tasks, the metric is defined as $\frac{n_c}{n}$, where n_c denotes the number of correctly matched nodes.

Baselines include project fixed-point algorithms such as DSPFP [27] and AIPFP [22, 27]; softassign-based algorithms such as GA [12] (based on (1)) and ASM [34]; optimal transport methods such as GWL [39] and S-GWL [38]; and a spectral-based algorithm, GRASP [16]. Among these, methods based on optimal transport and GRASP are designed for attribute-free graph matching tasks. Most baselines suffer from numerical overflow and accumulation of rounding error under low precision. Therefore, we omit their low-precision comparisons (see Appendix D for details). Many state-of-the-art algorithms, including Path Following [42], FGM [44], RRWM [2], PM [7], BGM [5], and MPM [3], do not scale well to large graphs (e.g., with more than 1000 nodes), and are thus not included in our large-scale graph matching comparisons.

7.1 Real-world pictures

In this experiment, the attributed graphs are constructed from a public dataset[3], containing eight sets of pictures. The dataset covers five common transformations: viewpoint change, scale change, image blur, JPEG compression and illumination. The numerical results are presented in Table 2.

[3] `http://www.robots.ox.ac.uk/~vgg/research/affine/`

Performance	Running Time							
Image Set	bark	boat	graf	wall	leuv	tree	ubc	bikes
DSPFP	9.1s	7.3s	8.8s	6.1s	5.8s	7.6s	6.1s	3.3s
AIPFP	44.3s	44.2s	84.4s	44.8s	26.3s	40.3s	34.3s	16.3s
GA	30.8s	31.0s	34.2s	29.7s	30.8s	29.8s	31.8s	16.8s
ASM	4.5s	4.5s	4.2s	5s	5s	3.8s	4.5s	3.2s
FRAM	**2.6**s	**2.1**s	**2.4**s	**2.3**s	**2.2**s	**2.5**s	**2.4**s	**1.1**s

Performance	Matching Error ($\times 10^4$)							
Image Set	bark	boat	graf	wall	leuv	tree	ubc	bikes
DSPFP	5.0	4.4	5.1	4.1	5.0	4.7	4.0	4.9
AIPFP	4.6	4.5	5.3	4.4	3.9	4.7	3.6	4.3
GA	4.9	5.3	6.4	6.6	4.2	6.3	3.4	4.6
ASM	4.6	4.4	4.9	4.2	**3.7**	**3.5**	3.3	**3.6**
FRAM	**4.2**	**4.0**	**4.6**	**3.6**	4.9	3.8	**3.1**	4.4

Table 2: Performance comparison in terms of (a) running time and (b) matching error on different image sets. The number of nodes is set to 1000 (*bike* set with 700 nodes). All algorithms are evaluated using double precision (FP64).

As a revolutionary version of DSPFP, FRAM achieves significant acceleration across all image sets. The average runtime of FRAM is 2.3s, compared to 6.5s for DSPFP, yielding an overall speedup of 2.8×. In addition to acceleration, FRAM consistently outperforms DSPFP regarding matching accuracy, demonstrating the effectiveness of the algorithmic design. Overall, FRAM achieves the best matching performance in more than half of the experiments while being nearly twice as fast as the second-fastest method, ASM.

7.2 House sequence

CMU house sequence[4] is a classic benchmark dataset. It consists of a sequence of images showing a toy house captured from different viewpoints. Figure 3 demonstrates that FRAM achieves the best performance in both speed and accuracy on the House sequence dataset. It runs 4.1× faster than DSPFP and 3.4× faster than ASM, while attaining the lowest matching error. These results clearly highlight FRAM's efficiency and effectiveness.

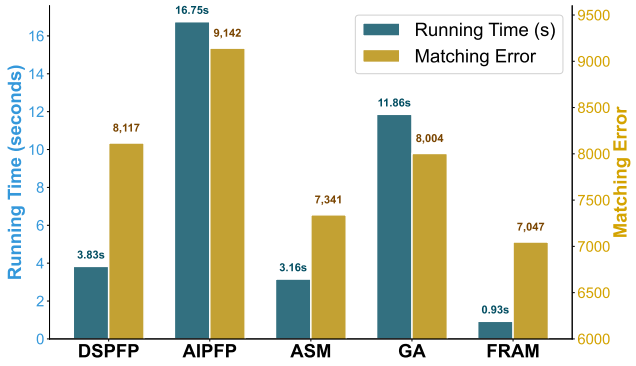

Figure 3: Comparisons between algorithms on graphs from the house sequence. All algorithms are evaluated using double precision (FP64).

7.3 Social networks

The social network, comprising 'circles' (or 'friends lists') from Facebook [23], contains 4039 users (nodes) and 88234 relations (edges). We compare different methods in matching networks with noisy versions at 5%, 15% and 25%. Table 3 shows that FRAM achieves the highest node accuracy across all noise levels while maintaining computational efficiency. FRAM achieves 4% higher accuracy than ASM (the second-best method) while running twice as fast. Although FRAM is slightly slower than DSPFP, it offers a substantial 15% improvement in accuracy, demonstrating a favorable trade-off between precision and efficiency.

[4]https://www.cs.cmu.edu/afs/cs/project/vision/vasc/idb/images/motion/house/

Social network	5% noise		15% noise		25% noise	
Methods	Acc	Time	Acc	Time	Acc	Time
S-GWL	26.4%	1204.1s	18.3%	1268.2s	17.9%	1295.8s
GWL	78.1%	3721.6s	68.4%	4271.3s	60.8%	4453.9s
DSPFP	79.7%	151.3s	68.3%	154.2s	62.2%	156.9s
GA	35.5%	793.2s	21.4%	761.7s	16.0%	832.6s
GRASP	37.9%	**63.6s**	20.3%	**67.4s**	15.7%	**71.3s**
ASM	91.1%	387.2s	88.4%	391.7s	85.7%	393.1s
AIPFP	68.6%	2705.5s	55.1%	2552.7s	47.8%	2513.8s
FRAM	**94.7%**	211.1s	**91.1%**	221.6s	**89.5%**	222.9s

Table 3: Results on Facebook network matching, which are evaluated using double precision (FP64).

7.4 Mixed-precision acceleration

This subsection analyzes the acceleration performance of mixed-precision design in FRAM across varying tasks. As demonstrated in Figure 4, the design shows markedly higher acceleration ratios for large-scale problems. Specifically, in the ubc(2000) matching task, mixed-precision design achieves (a) 12.7× speedup over standard GPU-FP64 implementations, and (b) a 371.4× acceleration compared to CPU-FP64 baselines. Conversely, for tasks with up to 1000 nodes, the observed speed-ups are below 4×, likely because the problem scale is insufficient to fully utilize the hardware's computational capacity. These observations are consistent with Amdahl's law: fixed computational overheads dominate runtime at small scales, significantly reducing achievable performance improvements.

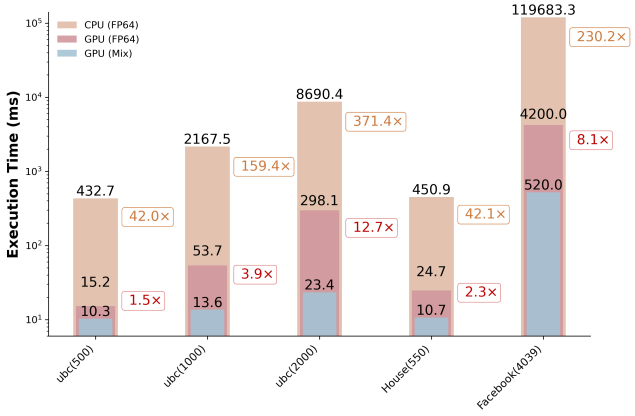

Figure 4: Runtime comparison of FRAM across different precisions and processors. The y-axis shows runtime (log scale), and the x-axis indicates datasets and their sizes. Red boxed numbers show the speedup of GPU mixed-precision over GPU double precision, and yellow boxed numbers show the speedup over CPU double precision.

8 Conclusion

In the context of graph matching, this study investigates the bias introduced by projection-based relaxations. To address this issue, we reformulate the projection step as a regularized linear assignment problem, providing a principled way to control the relaxation error. Building on this formulation, we propose a robust algorithm that achieves competitive accuracy while providing substantial speed advantages over existing baselines, including a significant improvement over the second-best method. On the computational side, we propose a theoretically grounded mixed-precision design. To the best of our knowledge, this is the first theoretically grounded mixed-precision design for graph matching. It achieves significant acceleration while maintaining numerical stability.

A limitation of this study lies in the empirical selection of the parameter θ, so we plan to develop an adaptive parameter selection strategy in future work. While our framework validates the effectiveness of mixed-precision computation, its computational efficiency can be improved. Future work may explore low-level compilation techniques to further optimize the implementation and unlock additional speed gains.

Acknowledgements

This work was partially supported by the Natural Science Foundation of China (12271047), the National Key Technologies Research and Development Program (2025YFG0202100), and the BNBU research fund (UICR0400008-21; UICR04202405-21). Thanks the support by the Interdisciplinary Intelligence Super Computer Center of Beijing Normal University at Zhuhai and the Guangdong Provincial Key Laboratory of Interdisciplinary Research and Application for Data Science (2022B1212010006).

References

[1] Florian Bernard, Christian Theobalt, and Michael Moeller. DS*: Tighter Lifting-Free Convex Relaxations for Quadratic Matching Problems. In *Proceedings of the IEEE Conference on Computer Vision and Pattern Recognition*, pages 4310–4319, 2018.

[2] Minsu Cho, Jungmin Lee, and Kyoung Mu Lee. Reweighted Random Walks for Graph Matching. In *European Conference on Computer Vision*, 2010.

[3] Minsu Cho, Jian Sun, Olivier Duchenne, and Jean Ponce. Finding matches in a haystack: A max-pooling strategy for graph matching in the presence of outliers. In *Proceedings of the IEEE Conference on Computer Vision and Pattern Recognition*, pages 2083–2090, 2014.

[4] Michael P Connolly, Nicholas J Higham, and Theo Mary. Stochastic rounding and its probabilistic backward error analysis. *SIAM Journal on Scientific Computing*, 43(1):A566–A585, 2021.

[5] Timothee Cour, Praveen Srinivasan, and Jianbo Shi. Balanced Graph Matching. *Advances in Neural Information Processing Systems*, 19, 2006.

[6] Nadav Dym, Haggai Maron, and Yaron Lipman. DS++: A Flexible, Scalable and Provably Tight Relaxation for Matching Problems. *ACM Transactions on Graphics*, 36(6):1–14, 2017.

[7] Amir Egozi, Yosi Keller, and Hugo Guterman. A probabilistic approach to spectral graph matching. *IEEE Transactions on Pattern Analysis and Machine Intelligence*, 35(1):18–27, 2012.

[8] Frank Emmert-Streib, Matthias Dehmer, and Yongtang Shi. Fifty years of graph matching, network alignment and network comparison. *Information Sciences*, 346:180–197, 2016.

[9] Fajwel Fogel, Rodolphe Jenatton, Francis Bach, and Alexandre d'Aspremont. Convex Relaxations for Permutation Problems. *Advances in Neural Information Processing Systems*, 26, 2013.

[10] Kexue Fu, Shaolei Liu, Xiaoyuan Luo, and Manning Wang. Robust point cloud registration framework based on deep graph matching. In *Proceedings of the IEEE/CVF Conference on Computer Vision and Pattern Recognition*, pages 8893–8902, 2021.

[11] Michael R Garey and David S Johnson. *Computers and Intractability: A Guide to the Theory of NP-Completeness*. WH Freeman & Co., 1979.

[12] Steven Gold and Anand Rangarajan. A graduated assignment algorithm for graph matching. *IEEE Transactions on Pattern Analysis and Machine Intelligence*, 18(4):377–388, 1996.

[13] David E Gordon, Joseph Hiatt, Mehdi Bouhaddou, Veronica V Rezelj, Svenja Ulferts, Hannes Braberg, Alexander S Jureka, Kirsten Obernier, Jeffrey Z Guo, Jyoti Batra, et al. Comparative host-coronavirus protein interaction networks reveal pan-viral disease mechanisms. *Science*, 370(6521):eabe9403, 2020.

[14] Jiawei He, Zehao Huang, Naiyan Wang, and Zhaoxiang Zhang. Learnable graph matching: Incorporating graph partitioning with deep feature learning for multiple object tracking. In *Proceedings of the IEEE/CVF Conference on Computer Vision and Pattern Recognition*, pages 5299–5309, 2021.

[15] Greg Henry, Ping Tak Peter Tang, and Alexander Heinecke. Leveraging the bfloat16 artificial intelligence datatype for higher-precision computations. In *2019 IEEE 26th Symposium on Computer Arithmetic (ARITH)*, pages 69–76. IEEE, 2019.

[16] Judith Hermanns, Konstantinos Skitsas, Anton Tsitsulin, Marina Munkhoeva, Alexander Kyster, Simon Nielsen, Alexander M Bronstein, Davide Mottin, and Panagiotis Karras. GRASP: Scalable Graph Alignment by Spectral Corresponding Functions. *ACM Transactions on Knowledge Discovery from Data*, 17(4):1–26, 2023.

[17] Nicholas J Higham and Theo Mary. Mixed precision algorithms in numerical linear algebra. *Acta Numerica*, 31:347–414, 2022.

[18] Harold W Kuhn. The Hungarian method for the assignment problem. *Naval Research Logistics Quarterly*, 2(1-2):83–97, 1955.

[19] Zixun Lan, Ye Ma, Limin Yu, Linglong Yuan, and Fei Ma. AEDNet: Adaptive Edge-Deleting Network For Subgraph Matching. *Pattern Recognition*, page 109033, 2022.

[20] Zixun Lan, Binjie Hong, Ye Ma, and Fei Ma. More Interpretable Graph Similarity Computation Via Maximum Common Subgraph Inference. *IEEE Transactions on Knowledge and Data Engineering*, pages 1–12, 2024.

[21] Marius Leordeanu and Martial Hebert. A spectral technique for correspondence problems using pairwise constraints. In *Tenth IEEE International Conference on Computer Vision (ICCV'05) Volume 1*, volume 2, pages 1482–1489. IEEE, 2005.

[22] Marius Leordeanu, Martial Hebert, and Rahul Sukthankar. An integer projected fixed point method for graph matching and map inference. In *Advances in Neural Information Processing Systems*, pages 1114–1122, 2009.

[23] Jure Leskovec and Andrej Krevl. SNAP Datasets: Stanford large network dataset collection. `http://snap.stanford.edu/data`, June 2014.

[24] Aixin Liu, Bei Feng, Bing Xue, Bingxuan Wang, Bochao Wu, Chengda Lu, Chenggang Zhao, Chengqi Deng, Chenyu Zhang, Chong Ruan, et al. Deepseek-v3 technical report. *arXiv preprint arXiv:2412.19437*, 2024.

[25] Chang Liu, Chenfei Lou, Runzhong Wang, Alan Yuhan Xi, Li Shen, and Junchi Yan. Deep neural network fusion via graph matching with applications to model ensemble and federated learning. In Kamalika Chaudhuri, Stefanie Jegelka, Le Song, Csaba Szepesvari, Gang Niu, and Sivan Sabato, editors, *Proceedings of the 39th International Conference on Machine Learning*, volume 162 of *Proceedings of Machine Learning Research*, pages 13857–13869. PMLR, 17–23 Jul 2022.

[26] David G Lowe. Distinctive image features from scale-invariant keypoints. *International Journal of Computer Vision*, 60(2):91–110, 2004.

[27] Yao Lu, Kaizhu Huang, and Cheng-Lin Liu. A fast projected fixed-point algorithm for large graph matching. *Pattern Recognition*, 60:971–982, 2016.

[28] Sharan Narang, Gregory Diamos, Erich Elsen, Paulius Micikevicius, Jonah Alben, David Garcia, Boris Ginsburg, Michael Houston, Oleksii Kuchaiev, Ganesh Venkatesh, et al. Mixed precision training. In *Int. Conf. on Learning Representation*, 2017.

[29] John Von Neumann. *Functional Operators, Volume II: The Geometry of Orthogonal Spaces*. Princeton University Press, Princeton, NJ, 1932. Reprinted in 1950.

[30] Duy M. H. Nguyen, Nghiem T. Diep, Trung Q. Nguyen, Hoang-Bao Le, Tai Nguyen, Tien Nguyen, TrungTin Nguyen, Nhat Ho, Pengtao Xie, Roger Wattenhofer, James Zhou, Daniel Sonntag, and Mathias Niepert. LoGra-Med: Long Context Multi-Graph Alignment for Medical Vision-Language Model, 2024. URL `https://arxiv.org/abs/2410.02615`.

[31] Sartaj Sahni. Computationally related problems. *SIAM Journal on computing*, 3(4):262–279, 1974.

[32] Sartaj Sahni and Teofilo Gonzalez. P-complete approximation problems. *Journal of the ACM (JACM)*, 23(3):555–565, 1976.

[33] Binrui Shen, Qiang Niu, and Shengxin Zhu. Fabricated Pictures Detection with Graph Matching. In *Proceedings of the 2020 2nd Asia Pacific Information Technology Conference*, pages 46–51, 2020.

[34] Binrui Shen, Qiang Niu, and Shengxin Zhu. Adaptive Softassign via Hadamard-Equipped Sinkhorn. In *Proceedings of the IEEE/CVF Conference on Computer Vision and Pattern Recognition*, pages 17638–17647, 2024.

[35] Binrui Shen, Qiang Niu, and Shengxin Zhu. Lightning graph matching. *Journal of Computational and Applied Mathematics*, 454:116189, 2025.

[36] Ziying Song, Haiyue Wei, Lin Bai, Lei Yang, and Caiyan Jia. Graphalign: Enhancing accurate feature alignment by graph matching for multi-modal 3d object detection. In *Proceedings of the IEEE/CVF International Conference on Computer Vision*, pages 3358–3369, 2023.

[37] Vogelstein, Joshua T and Conroy, John M and Lyzinski, Vince and Podrazik, Louis J and Kratzer, Steven G and Harley, Eric T and Fishkind, Donniell E and Vogelstein, R Jacob and Priebe, Carey E. Fast Approximate Quadratic Programming for Graph Matching. *PLOS one*, 10(4):e0121002, 2015.

[38] Hongteng Xu, Dixin Luo, and Lawrence Carin. Scalable gromov-wasserstein learning for graph partitioning and matching. In *Advances in Neural Information Processing Systems*, volume 32, 2019.

[39] Hongteng Xu, Dixin Luo, Hongyuan Zha, and Lawrence Carin Duke. Gromov-wasserstein learning for graph matching and node embedding. In *International Conference on Machine Learning*, pages 6932–6941. PMLR, 2019.

[40] Kun Xu, Liwei Wang, Mo Yu, Yansong Feng, Yan Song, Zhiguo Wang, and Dong Yu. Cross-lingual Knowledge Graph Alignment via Graph Matching Neural Network. In *Proceedings of the 57th Annual Meeting of the Association for Computational Linguistics*, pages 3156–3161, 2019.

[41] Junchi Yan, Xu-Cheng Yin, Weiyao Lin, Cheng Deng, Hongyuan Zha, and Xiaokang Yang. A short survey of recent advances in graph matching. In *Proceedings of the 2016 ACM on international conference on multimedia retrieval*, pages 167–174, 2016.

[42] Mikhail Zaslavskiy, Francis Bach, and Jean-Philippe Vert. A path following algorithm for the graph matching problem. *IEEE Transactions on Pattern Analysis and Machine Intelligence*, 31 (12):2227–2242, 2008.

[43] Ron Zass and Amnon Shashua. Doubly stochastic normalization for spectral clustering. *Advances in Neural Information Processing Systems*, 19, 2006.

[44] Feng Zhou and Fernando De la Torre. Factorized Graph Matching. *IEEE Transactions on Pattern Analysis and Machine Intelligence*, 38(9):1774–1789, 2015.

A Notations

The common symbols are summarized in Table A.

Table 4: Symbols and Notations.

Symbol	Definition
$G, \tilde{G}$	matching graphs
$A, \tilde{A}$	edge attribute matrices of G and $\tilde{G}$
$F, \tilde{F}$	node attribute matrices of G and $\tilde{G}$
$n, \tilde{n}$	number of nodes of G and $\tilde{G}$
M	matching matrix
$\Pi_{n\times n}$	the set of $n \times n$ permutation matrices
$\mathcal{D}_{n\times n}$	the set of $n \times n$ doubly stochastic matrices
$\mathbf{1}$,$\mathbf{0}$	a column vector of all 1s,0s
$\mathrm{tr}(\cdot)$	trace
$\langle \cdot, \cdot \rangle$	Frobenius inner product
$\|\cdot\|_F$	Frobenius norm
θ	the parameter in FRA
α	the step-size parameter
FP8/16/32/64	8/16/32/64-bit Floating Point
TF32	TensorFloat 32

B Convergence Criterions

B.1 Convergence criterion of SDSN

We recall the SDSN projection steps below:

$$\tilde{X}^{(k)} = \mathcal{P}_1\left(X^{(k-1)}\right), \;\; X^{(k)} = \mathcal{P}_2\left(\tilde{X}^{(k)}\right),$$

$$\mathcal{P}_1(X) = X + \left(\frac{I}{n} + \frac{\mathbf{1}^T X \mathbf{1}}{n^2} I - \frac{\mathbf{X}}{n}\right)\mathbf{1}\mathbf{1}^T - \frac{\mathbf{1}\mathbf{1}^{\mathbf{T}}\mathbf{X}}{n}, \qquad \mathcal{P}_2(X) = \frac{X + |X|}{2}.$$

Before the non-negative projection, the updated matrix satisfies

$$\sum_{i,j} \tilde{X}_{ij}^{(k)} = \sum_{\tilde{X}_{ij}^{(k)}>0} \tilde{X}_{ij}^{(k)} + \sum_{\tilde{X}_{ij}^{(k)}<0} \tilde{X}_{ij}^{(k)} = n. \tag{22}$$

After applying the non-negative projection (all negative elements are set to 0), we obtain

$$\sum_{i,j} X_{ij}^{(k)} = \sum_{\tilde{X}_{ij}^{(k)}>0} \tilde{X}_{ij}^{(k)} = n + \sum_{\tilde{X}_{ij}^{(k)}<0} |\tilde{X}_{ij}^{(k)}|. \tag{23}$$

Since $\sum_{i,j} X_{ij}^{(k)}$ converges to n,

$$\sum_{\tilde{X}_{ij}^{(k)}<0} |\tilde{X}_{ij}^{(k)}| = \sum_{i,j} X_{ij}^{(k)} - n \tag{24}$$

is natural to represent the residual. Moreover, the von Neumann successive projection lemma [29] guarantees that this distance decreases monotonically over successive iterations. Therefore, we define a **dimensional scaled error** as

$$\gamma(X^{(k)}) = \frac{1}{n}\sum_{i,j} X_{ij}^{(k)} - 1 = \frac{\mathbf{1}^T X^{(k)} \mathbf{1}}{n} - 1, \tag{25}$$

where normalization by n ensures applicability to matrices of any size. Furthermore, since $\mathbf{1}^T X^{(k-1)} \mathbf{1}$ is computed in $\mathcal{P}_1(\cdot)$, we can avoid the computation for the error by approximately using $\gamma(X^{(k-1)})$ in k-th iteration.

B.2 Convergence criterion of the matching algorithm

The matching algorithm in DSPFP [27] adopts the following original convergence criterion:

$$\max\left(\left|\frac{N^{(t)}}{\max(N^{(t)})}-\frac{N^{(t-1)}}{\max(N^{(t-1)})}\right|\right), \tag{26}$$

which was also adopted by the ASM [34]. This metric primarily captures local fluctuations between the successive iterations. To better characterize the global structural evolution, we adopt the following **normalized Frobenius criterion**:

$$\delta^{(t)}=\frac{\|N^{(t)}-N^{(t-1)}\|_F}{\|N^{(t)}\|_F}. \tag{27}$$

This criterion demonstrates enhanced suitability for our framework due to two principal considerations: (1) The Frobenius norm inherently aligns with the FRA and the objective formulation, ensuring mathematical consistency throughout the optimization process. (2) The normalization scheme provides a scale-invariant measurement of the variation of the solution trajectory.

C Proofs in Section 4

Theorem 1. *The solution to the scaled doubly stochastic projection problem*

$$D_X^\theta=\arg\min_{D\in\mathcal{D}_{n\times n}}\|D-\tfrac{\theta}{2}X\|_F^2 \tag{28}$$

is equivalent to the solution of a Frobenius-regularized linear assignment problem:

$$D_X^\theta=\arg\max_{D\in\mathcal{D}_{n\times n}}\Gamma^\theta(X),\quad \Gamma^\theta(X)=\langle D,X\rangle-\tfrac{1}{\theta}\langle D,D\rangle. \tag{29}$$

Proof. The squared Frobenius norm can be expanded as:

$$\|D-\frac{\theta}{2}X\|_F^2=\langle D,D\rangle-2\langle D,\frac{\theta}{2}X\rangle+\langle\frac{\theta}{2}X,\frac{\theta}{2}X\rangle. \tag{30}$$

Since the term $\langle\frac{\theta}{2}X,\frac{\theta}{2}X\rangle$ is a constant with respect to D, it does not affect the optimization. Thus, the objective simplifies to:

$$D_X^\theta=\arg\min_{D\in\mathcal{D}_{n\times n}}\langle D,D\rangle-\theta\langle D,X\rangle. \tag{31}$$

As a result, the problem reduces to:

$$D_X^\theta=\arg\max_{D\in\mathcal{D}_{n\times n}}\langle D,X\rangle-\frac{1}{\theta}\langle D,D\rangle. \tag{32}$$

□

Proposition 1. *For a nonnegative matrix $X\in\mathbb{R}^{n\times n}$, the following inequality holds:*

$$\epsilon_X^\theta\le\frac{1}{\theta}. \tag{33}$$

Proof. Since D_X^θ is the maximizer of $\Gamma^\theta(X)$, we have

$$\Gamma^\theta(D_X^\theta)\ge\Gamma^\theta(D_X^\infty), \tag{34}$$

where D_X^∞ is a maximizer of the unperturbed problem $\max_{D\in\mathcal{D}_{n\times n}}\langle D,X\rangle$.

Expanding the inequality gives:

$$\langle D_X^\theta,X\rangle-\frac{1}{\theta}\langle D_X^\theta,D_X^\theta\rangle\ge\langle D_X^\infty,X\rangle-\frac{1}{\theta}\langle D_X^\infty,D_X^\infty\rangle. \tag{35}$$

Rearranging terms, we have:

$$\langle D_X^\theta,X\rangle-\langle D_X^\infty,X\rangle\ge\frac{1}{\theta}\big(\langle D_X^\theta,D_X^\theta\rangle-\langle D_X^\infty,D_X^\infty\rangle\big). \tag{36}$$

In particular, the maximum of $\langle D_X^\infty, D_X^\infty \rangle$ is n when D_X^∞ is a permutation matrix. Therefore, we have $\langle D_X^\infty, D_X^\infty \rangle \leq n$ for general cases.

$$\langle D_X^\theta, X \rangle - \langle D_X^\infty, X \rangle \geq \frac{1}{\theta}(\langle D_X^\theta, D_X^\theta \rangle - n). \tag{37}$$

Taking the negative of both sides,

$$\langle D_X^\infty, X \rangle - \langle D_X^\theta, X \rangle \leq \frac{1}{\theta}(n - \langle D_X^\theta, D_X^\theta \rangle). \tag{38}$$

Note that $D_X^\theta \in \mathcal{D}_{n\times n}$ is doubly stochastic, so $1 \leq \langle D_X^\theta, D_X^\theta \rangle \leq n$ (The inner product achieves its maximum value when D_X^θ is a permutation matrix, while attaining its minimum value under the condition that all elements of D_X^θ are $\frac{1}{n}$). Therefore,

$$\langle D_X^\infty, X \rangle - \langle D_X^\theta, X \rangle \leq \frac{n-1}{\theta}, \tag{39}$$

which completes the proof. □

Theorem 2. *Let $X \in \mathbb{R}_+^{n\times n}$ and $\mathcal{F}$ be the convex hull of the optimal permutation matrices for the linear assignment problem with X. As $\theta \to \infty$, the matrix D_X^θ converges to a unique matrix $D^* \in \mathcal{F}$, where D^* is the unique solution to* $\min_{D\in\mathcal{F}} \frac{1}{\theta}\langle D, D \rangle$.

Proof. We prove the theorem in two steps: (1) D_X^∞ lies on the face $\mathcal{F}$, and (2) D_X^∞ must equal D^*.

Step 1. Since D_X^θ is defined as the maximizer of

$$\Gamma^\theta(D) = \langle D, X \rangle - \frac{1}{\theta}\langle D, D \rangle, \tag{40}$$

we have

$$\Gamma^\theta(D_X^\theta) \geq \Gamma^\theta(D^*), \tag{41}$$

which implies

$$\langle D_X^\theta, X \rangle - \frac{1}{\theta}\langle D_X^\theta, D_X^\theta \rangle \geq \langle D^*, X \rangle - \frac{1}{\theta}\langle D^*, D^* \rangle. \tag{42}$$

As $\theta \to \infty$, we have

$$\frac{1}{\theta}\langle D_X^\theta, D_X^\theta \rangle \to 0 \quad \text{and} \quad \frac{1}{\theta}\langle D^*, D^* \rangle \to 0. \tag{43}$$

Taking the limit, we get

$$\lim_{\theta\to\infty} \langle D_X^\theta, X \rangle \geq \langle D^*, X \rangle. \tag{44}$$

Since D^* is the optimal solution to the linear assignment problem, for any $D \in \mathcal{D}_{n\times n}$,

$$\langle D, X \rangle \leq \langle D^*, X \rangle. \tag{45}$$

In particular,

$$\langle D_X^\theta, X \rangle \leq \langle D^*, X \rangle. \tag{46}$$

Combining both inequalities, we obtain

$$\lim_{\theta\to\infty} \langle D_X^\theta, X \rangle = \langle D^*, X \rangle, \tag{47}$$

which means D_X^∞ lies in the face $\mathcal{F}$.

Step 2. For each fixed θ, the objective $\Gamma^\theta(D)$ is strictly concave in D due to the quadratic term $-\frac{1}{\theta}\langle D, D \rangle$. Strict concavity ensures that for large θ, the maximizer of $\Gamma^\theta(D)$ is unique.

Suppose, for the sake of contradiction, that $D_X^\infty \neq D^*$. Since both are in $\mathcal{F}$, we have

$$\langle D_X^\infty, X \rangle = \langle D^*, X \rangle. \tag{48}$$

If D_X^∞ were distinct from D^*, then as $\theta \to \infty$, the perturbed objective $\Gamma^\theta(D)$ would admit at least two different maximizers (D_X^∞ and D^*) with the same objective value. This contradicts the uniqueness guaranteed by strict concavity. Therefore, D_X^∞ must coincide with D^*.

Since the entire sequence D_X^θ is bounded and any convergent subsequence converges to D^*, it follows that

$$D_X^\theta \to D^* \text{ as } \theta \to \infty. \tag{49}$$

This establishes the desired convergence. □

Proposition 2. *As $\theta \to 0$, the matrix D_X^θ converges to the matrix $\frac{\mathbf{1}\mathbf{1}^T}{n}$.*

Proof. As $\theta \to 0$, the matrix D_X^θ exhibits the limiting behavior:

$$\lim_{\theta \to 0} D_X^\theta = \arg \min_{D \in \mathcal{D}_{n \times n}} \langle D, D \rangle = \sum D_{ij}^2. \tag{50}$$

Since $\sum D_{ij} = n$, $\sum D_{ij}^2$ achieve minimum when all entries are equal to $1/n$. Consequently,

$$\lim_{\theta \to 0} D_X^\theta = \frac{\mathbf{1}\mathbf{1}^T}{n}. \tag{51}$$

□

Proposition 3. *For $X \in \mathbb{R}_+^{n \times n}$, the SDSN algorithm requires*

$$\left\lceil \ln\left(\frac{\epsilon}{\theta(\|X\|_F + n)}\right) \frac{1}{\ln(c)} \right\rceil$$

iterations to produce a solution X^* that satisfies $\|X^* - D_X^\theta\|_F < \epsilon$ where D_X^θ is the exact solution and $c \in (0, 1)$ is the convergence rate constant of the DSN algorithm.

Proof.

$$X_{k+1} = \mathcal{P}_1 \mathcal{P}_2(X_k) \tag{52}$$

where $\mathcal{P}_1$ and $\mathcal{P}_2$ denote projection operators maintaining the constraint $X_k \mathbf{1} = (\mathbf{1}^T X_k)^T = \mathbf{1}$. This operation can be explicitly expressed as:

$$X_{k+1} = \mathcal{P}_1 \left(X_k + |X_k|\right) \tag{53}$$

with the absolute value operation applied element-wise to matrix entries. Expanding the projection operators yields the detailed formulation:

$$X_{k+1} = \frac{1}{2}(X_k + |X_k|) + \frac{\mathbf{1}^T[\frac{1}{2}(X_k + |X_k|)]\mathbf{1}}{n^2}\mathbf{1}\mathbf{1}^T - \frac{1}{n}[\frac{1}{2}(X_k + |X_k|)]\mathbf{1}\mathbf{1}^T - \frac{1}{n}\mathbf{1}\mathbf{1}^T[\frac{1}{2}(X_k + |X_k|)] + \frac{1}{n}\mathbf{1}\mathbf{1}^T. \tag{54}$$

Through vectorization and Kronecker product analysis, we transform the matrix equation into its vector form:

$$\text{vec}(X_{k+1}) = A \,\text{vec}\left(|X_k| + X_k\right) + \frac{1}{n}\text{vec}\left(\mathbf{1}\mathbf{1}^T\right) \tag{55}$$

where $A = \frac{1}{2}(I - \frac{1}{n}\mathbf{1}\mathbf{1}^T) \otimes (I - \frac{1}{n}\mathbf{1}\mathbf{1}^T)$ possesses a spectral radius of $\frac{1}{2}$. Defining the error vector $e_k = \text{vec}(X_k) - \text{vec}(X_*)$ for solution matrix X_*, we derive the error propagation relationship:

$$e_{k+1} = A \,\text{vec}\left(|X_k| - X_*\right) + Ae_k \tag{56}$$

Applying norm inequalities and leveraging the spectral properties of A, we obtain:

$$\|e_{k+1}\| \leq \frac{1}{2}\left(\mathrm{c}_k \|e_k\| + \|e_k\|\right) = c\|e_k\| \tag{57}$$

where $c = \sup_{1:k}\{\frac{\mathrm{c}_k + 1}{2}\} < 1$ establishes the linear convergence rate.

Considering scaled initial conditions $\theta\mathbf{X}$, the first iteration error becomes $\|e_1\| = \|\theta \cdot e_0\|$. For k iterations with scaling factor θ, the error evolution follows:

$$\|e_k\| = \|\theta \cdot c^k \cdot e_0\| \tag{58}$$

The ϵ-accuracy requirement $\|\theta \cdot c^{k'} \cdot e_0\| \leq \epsilon$ leads to the logarithmic relationship:

$$\ln \theta + k' \ln c + \ln \|e_0\| \leq \ln \epsilon \tag{59}$$

Solving for the required iterations yields:

$$k' \geq \frac{\ln(\epsilon/\theta) + \ln(\epsilon/\|e_0\|)}{\ln c} = \frac{\ln\left(\epsilon/(\theta\|e_0\|)\right)}{\ln c} \tag{60}$$

Given the initial error bound $\|e_0\| = \|X\|_F + n \leq \|X\|_F + n$, we finalize the iteration complexity:

$$k' \geq \frac{\ln\left(\frac{\epsilon}{\theta(\|\mathbf{X}\|_F + n)}\right)}{\ln c} \tag{61}$$

This demonstrates the logarithmic relationship between the scaling factor θ and the required iterations to maintain solution accuracy, completing the proof. □

Lemma 1. *The closed-form solution to the optimization problem*

$$\mathcal{P}_3(X) = \arg\min_{Y} \|X - Y\|_F^2, \text{ s.t. } Y\mathbf{1} = Y^T\mathbf{1} = \mathbf{0} \tag{62}$$

is given by:

$$\mathcal{P}_3(X) = X + \left(\frac{1}{n^2}\mathbf{1}^T X\mathbf{1} - \frac{1}{n}X\right)\mathbf{1}\mathbf{1}^T - \frac{1}{n}\mathbf{1}\mathbf{1}^T X. \tag{63}$$

Proof. The Lagrangian corresponding to the problem takes the form:

$$L(Y, \mu_1, \mu_2) = \mathrm{tr}(YY^T - 2XY) - \mu_1^T Y\mathbf{1} - \mu_2^T Y^T. \tag{64}$$

By differentiating (64), we can obtain the following:

$$\frac{\partial L}{\partial Y} = Y - X - \mu_1\mathbf{1}^T - \mathbf{1}\mu_2^T, \quad \frac{\partial L}{\partial \mu_1} = Y\mathbf{1}, \quad \frac{\partial L}{\partial \mu_2} = Y^T\mathbf{1}. \tag{65}$$

Thus, let $\frac{\partial L}{\partial Y} = 0$, we have:

$$Y = X + \mu_1\mathbf{1}^T + \mathbf{1}\mu_2^T. \tag{66}$$

Applying $\mathbf{1}$ to both sides of the equation above, we get:

$$0 = X\mathbf{1} + n\mu_1 + \mathbf{1}\mu_2^T\mathbf{1}. \tag{67}$$

Multiplying both sides of (67) by n, we get:

$$\mathbf{0} = nX\mathbf{1} + n^2\mu_1 + n\mathbf{1}\mu_2^T\mathbf{1}. \tag{68}$$

Multiplying both sides of (68) by $\mathbf{1}\mathbf{1}^T$, we get:

$$\mathbf{0} = \mathbf{1}\mathbf{1}^T X\mathbf{1} + n\mathbf{1}\mathbf{1}^T\mu_1 + n\mathbf{1}\mu_2^T\mathbf{1}. \tag{69}$$

Subtracting (68) and (69), we obtain:

$$(nI - \mathbf{1}\mathbf{1}^T)X\mathbf{1} + n(nI - \mathbf{1}\mathbf{1}^T)\mu_1 = 0. \tag{70}$$

Solving this equation, we find:

$$\mu_1 = \frac{1}{n}X\mathbf{1} - k_1\mathbf{1}, \quad \mu_2 = -\frac{1}{n}X^T\mathbf{1} - k_2\mathbf{1}, \tag{71}$$

where $k_1, k_2 \in \mathbb{R}$.

Substituting the results into (64), we rewrite the Lagrangian as:

$$L(Y, k_1, k_2) = \mathrm{tr}(FF^T - 2XF) + (\frac{1}{n}X\mathbf{1} + k_1\mathbf{1})^T Y\mathbf{1} + (\frac{1}{n}X^T\mathbf{1} + k_2\mathbf{1})^T Y^T. \tag{72}$$

Finally, setting $\frac{\partial L}{\partial Y} = \frac{\partial L}{\partial k_1} = \frac{\partial L}{\partial k_2} = 0$, we solve for Y:

$$Y = X + \left(\frac{\mathbf{1}^T X\mathbf{1}}{n^2}I - \frac{1}{n}X\right)\mathbf{1}\mathbf{1}^T - \frac{1}{n}\mathbf{1}\mathbf{1}^T X, \tag{73}$$

which completes the proof. □

Theorem 3. *In the SDSN algorithm, the k-th iterate X_k can be split as $X_k = \hat{X}_k + \Delta X_k$, where ΔX_k represents the rounding error. Then, the projection operator satisfies*

$$\mathcal{P}_1(X_k) = \mathcal{P}_1(\hat{X}_k) + \mathcal{P}_3(\Delta X_k),$$

where $\mathcal{P}_3(\Delta X)$ is the solution to the following minimization problem:

$$\mathcal{P}_3(\Delta X) = \arg\min_{Y} \|\Delta X - Y\|_F^2, \quad \textit{s.t. } Y\mathbf{1} = \mathbf{0},\ Y^\top \mathbf{1} = \mathbf{0}.$$

The subsequent transformations of the error term ΔX_k can be expressed as

$$\mathcal{P}_2\mathcal{P}_3 \cdots \mathcal{P}_2\mathcal{P}_3(\Delta X_k),$$

which asymptotically converges to the zero matrix $\mathbf{0}_{n\times n}$.

Proof. In SDSN calculations, the nonnegativity-enforcing part can be computed entirely in low precision, so this error analysis focuses on the first component $\mathcal{P}_1$ (19). To examine the behavior of the rounding error ΔX_k during iterations, we split X_k, the variable at the k-th iteration, as

$$X_k = \hat{X}_k + \Delta X_k. \tag{74}$$

Then, $\mathcal{P}_1(X_k)$ becomes

$$\begin{aligned}
&\left(\frac{I}{n} + \frac{1^T(\hat{X}_k + \Delta X_k)1I}{n^2} - \frac{(\hat{X}_k + \Delta X_k)1}{n}\right)11^T + \hat{X}_k + \Delta X_k - \frac{1}{n}11^T(\hat{X}_k + \Delta X_k) \qquad (75)\\
&= \underbrace{\hat{X}_k + \left(\frac{I}{n} + \frac{1^T\hat{X}_k 1I}{n^2} - \frac{\hat{X}_k}{n}\right)11^T - \frac{11^T\hat{X}_k}{n}}_{\mathcal{P}_1(\hat{X}_k)} + \underbrace{\Delta X_k + \left(\frac{1^T\Delta X_k 1}{n^2}I - \frac{\Delta X_k}{n}\right)11^T - \frac{11^T\Delta X_k}{n}}_{\Delta T_k}.
\end{aligned}$$

Lemma 1 establishes that $\Delta T_k = \mathcal{P}_3(\Delta X_k)$, so the subsequent transformation of ΔX_k can be represented as

$$\mathcal{P}_2\mathcal{P}_3 \cdots \mathcal{P}_2\mathcal{P}_3(\Delta X_k).$$

Through this process, the propagation of this rounding error ultimately converges to $\mathbf{0}_{n\times n}$ to satisfy the constraints imposed by both $\mathcal{P}_2(\cdot)$ and $\mathcal{P}_3(\cdot)$.

□

D Details of the Mixed-Precision Design

Algorithm 1 Frobenius-Regularized Assignment Matching (FRAM)

Require: $A, \tilde{A}, K, \lambda, \alpha, \theta, \delta_{th}$
Initial $X^{(0)} = \mathbf{0}_{n\times\tilde{n}}$
$c = \max(A, \tilde{A}, K)$ ▷ FP64
$A = A/\sqrt{c},\ \tilde{A} = \tilde{A}/\sqrt{c},\ K = K/\sqrt{c}$ ▷ FP64
while $\delta^{(t)} > \delta_{th}$ **do**
    $X^{(t)} = AN^{(t-1)}\tilde{A} + \lambda K$ ▷ TF32
    $D^{(t)} = \text{SDSN}(X^{(t)}, \theta)$ ▷ FP32
    $N^{(t)} = (1-\alpha)N^{(t-1)} + \alpha D^{(t)}$ ▷ FP64
    $\delta^{(t)} = \|N^{(t)} - N^{(t-1)}\|_F / \|N^{(t)}\|_F$ ▷ FP64
end while
$Discretize\ N\ to\ obtain\ M$ ▷ FP64
return Matching matrix M

Implementation details of the mixed-precision design.

Algorithm 1 employs mixed-precision design to improve computational efficiency while maintaining numerical stability, with precision for each operation specified via inline annotations. It starts by

normalizing matrices A, $\tilde{A}$, and K in steps 2-3 using FP64 to prevent overflow and ensure input consistency, enabling subsequent low-precision acceleration.

Step 5 employs TF32 (which is computationally similar to FP16) for critical computations. This strategy strikes a balance between performance and accuracy: it utilizes high-throughput GPU fused multiply-add operations while keeping precision loss within acceptable limits, as proven in Theorem 3. In contrast, further reducing the precision risks numerical instability due to inadequate accuracy.

Step 6 then switches to FP32 to maintain consistency, as FP16 would introduce additional truncation error, reducing accuracy by approximately 5% without increasing iterations. In contrast, FP32 maintains nearly the same number of iterations as FP64, balancing efficiency and precision.

Finally, step 7 reverts to FP64 for high-precision iterative updates, compensating for earlier precision trade-offs. Steps 8 and 10 continue in FP64 to ensure final output accuracy. This precision hierarchy accelerates performance in preconditioned computations while maintaining the reliability required for assignment matching tasks.

Introduction to different data type.

Data Type	Bits	Range	Precision	FLOPs (RTX 4080)
FP32	32	$[-10^{38}, 10^{38}]$	10^{-6}	52.2 TeraFLOPS
TF32	19	$[-10^{38}, 10^{38}]$	10^{-3}	209 TeraFLOPS
FP64	64	$[-10^{308}, 10^{308}]$	10^{-16}	0.82 TeraFLOPS

Table 5: Characteristics of FP32, TF32, and FP64 floating-point formats. The listed ranges are approximate, based on the IEEE 754 standard. The FLOPs column reports the theoretical peak performance (in TeraFLOPS) achieved by the NVIDIA RTX 4080 GPU for each format. Here, 1 TeraFLOPS equals 10^{12} floating-point operations per second, providing a standard measure of compute performance.

Why were competing algorithms not evaluated in lower precision settings? Mixed precision requires careful theoretical justification to ensure robustness against truncation errors and to preserve numerical stability. Not all baseline methods are robust in this regard. In particular, GA, S-GWL, GWL, and ASM all involve exponential operators, which are prone to numerical instability. For example, even in double precision, the default parameter settings in S-GWL can already cause numerical overflow, as documented in Appendix F of [34], making single-precision computation even more problematic. Among the remaining baselines, though AIPFP is comparatively more tolerant of reduced precision, it suffers from slow runtime; GRASP is inherently sensitive to noise. Lowering the precision does not alleviate their main limitations.

E Graphs from Images

The construction consists of three primary steps. (1) Node extraction: SIFT [26] extracts key points as potential nodes and computes the nodes' attributes; (2) Node selection: select the nodes that exhibit a high degree of similarity (i.e., the inner product of feature vectors) to all candidate nodes of the other graph. (3) Edge attribute calculation: nodes form a fully connected graph weighted by inter-node Euclidean distances.

Real-world images. The graphs are constructed as described in the previous paragraph. The number of nodes is set to 1000 (For the *bike* set, we only record the results for the first three pictures with 700 nodes, as the other images lack sufficient keypoints.). The running time and matching error are computed by averaging the results over five matching pairs (1 vs. 2, 2 vs. 3, ..., 5 vs. 6) from the same image set.

House sequence is a widely used benchmark dataset consisting of 111 grayscale images of a toy house taken from different viewpoints. The graphs are constructed as described in the previous paragraph, but without node attributes, to evaluate the algorithms from a different perspective. Matching pairs consist of the first image and subsequent images with 5 image sequence gaps (such as image 1 vs. image 6 and so on).

F Discussion of the regularization parameter

We evaluated the impact of the parameter θ on the FRAM algorithm across different types of tasks, as shown in Table 6. Overall, the algorithm's performance increases as the parameter grows, but the improvements follow a pattern of diminishing marginal effect, while an excessively large θ may lead to a slight degradation in performance. For tasks with attributed information, relatively small values of θ are sufficient to achieve good performance. In contrast, for more challenging tasks without attributed information, larger values of θ are required to achieve the best performance.

House (attributed edges)			**Bark** (attributed edges and nodes)			**Facebook Network**		
θ	Time (sec)	Error ($\times 10^3$)	θ	Time (sec)	Error ($\times 10^4$)	θ	Time (sec)	Node Accuracy
0.1	0.4	16.4	0.1	0.5	5.4	1	165	69.26%
0.5	0.6	7.3	0.5	0.6	4.1	5	192	85.92%
1	0.7	7.2	1	0.9	4.2	10	222	91.69%
2	0.9	7.0	2	1.1	4.2	15	246	93.48%
4	1.2	7.1	4	1.2	4.3	20	263	93.98%

Table 6: Influence of the parameter θ on algorithmic performance across diverse graph types.

NeurIPS Paper Checklist

1. **Claims**

   Question: Do the main claims made in the abstract and introduction accurately reflect the paper's contributions and scope?

   Answer: [Yes]

   Justification: We provide detailed proofs and many numerical experiments for what we claimed in the abstract.

   Guidelines:

   - The answer NA means that the abstract and introduction do not include the claims made in the paper.
   - The abstract and/or introduction should clearly state the claims made, including the contributions made in the paper and important assumptions and limitations. A No or NA answer to this question will not be perceived well by the reviewers.
   - The claims made should match theoretical and experimental results, and reflect how much the results can be expected to generalize to other settings.
   - It is fine to include aspirational goals as motivation as long as it is clear that these goals are not attained by the paper.

2. **Limitations**

   Question: Does the paper discuss the limitations of the work performed by the authors?

   Answer: [Yes]

   Justification: As mentioned in the conclusion, the parameter θ is set empirically, and the implementation of mixed-precision acceleration remains preliminary.

   Guidelines:

   - The answer NA means that the paper has no limitation while the answer No means that the paper has limitations, but those are not discussed in the paper.
   - The authors are encouraged to create a separate "Limitations" section in their paper.
   - The paper should point out any strong assumptions and how robust the results are to violations of these assumptions (e.g., independence assumptions, noiseless settings, model well-specification, asymptotic approximations only holding locally). The authors should reflect on how these assumptions might be violated in practice and what the implications would be.
   - The authors should reflect on the scope of the claims made, e.g., if the approach was only tested on a few datasets or with a few runs. In general, empirical results often depend on implicit assumptions, which should be articulated.
   - The authors should reflect on the factors that influence the performance of the approach. For example, a facial recognition algorithm may perform poorly when image resolution is low or images are taken in low lighting. Or a speech-to-text system might not be used reliably to provide closed captions for online lectures because it fails to handle technical jargon.
   - The authors should discuss the computational efficiency of the proposed algorithms and how they scale with dataset size.
   - If applicable, the authors should discuss possible limitations of their approach to address problems of privacy and fairness.
   - While the authors might fear that complete honesty about limitations might be used by reviewers as grounds for rejection, a worse outcome might be that reviewers discover limitations that aren't acknowledged in the paper. The authors should use their best judgment and recognize that individual actions in favor of transparency play an important role in developing norms that preserve the integrity of the community. Reviewers will be specifically instructed to not penalize honesty concerning limitations.

3. **Theory assumptions and proofs**

   Question: For each theoretical result, does the paper provide the full set of assumptions and a complete (and correct) proof?

Answer: [Yes]

Justification: We have clearly listed the assumptions of each theorem, and have provided the proof in the appendix

Guidelines:

- The answer NA means that the paper does not include theoretical results.
- All the theorems, formulas, and proofs in the paper should be numbered and cross-referenced.
- All assumptions should be clearly stated or referenced in the statement of any theorems.
- The proofs can either appear in the main paper or the supplemental material, but if they appear in the supplemental material, the authors are encouraged to provide a short proof sketch to provide intuition.
- Inversely, any informal proof provided in the core of the paper should be complemented by formal proofs provided in appendix or supplemental material.
- Theorems and Lemmas that the proof relies upon should be properly referenced.

4. **Experimental result reproducibility**

   Question: Does the paper fully disclose all the information needed to reproduce the main experimental results of the paper to the extent that it affects the main claims and/or conclusions of the paper (regardless of whether the code and data are provided or not)?

   Answer: [Yes]

   Justification: We have provided the code to reproduce the experiments in the article.

   Guidelines:

   - The answer NA means that the paper does not include experiments.
   - If the paper includes experiments, a No answer to this question will not be perceived well by the reviewers: Making the paper reproducible is important, regardless of whether the code and data are provided or not.
   - If the contribution is a dataset and/or model, the authors should describe the steps taken to make their results reproducible or verifiable.
   - Depending on the contribution, reproducibility can be accomplished in various ways. For example, if the contribution is a novel architecture, describing the architecture fully might suffice, or if the contribution is a specific model and empirical evaluation, it may be necessary to either make it possible for others to replicate the model with the same dataset, or provide access to the model. In general. releasing code and data is often one good way to accomplish this, but reproducibility can also be provided via detailed instructions for how to replicate the results, access to a hosted model (e.g., in the case of a large language model), releasing of a model checkpoint, or other means that are appropriate to the research performed.
   - While NeurIPS does not require releasing code, the conference does require all submissions to provide some reasonable avenue for reproducibility, which may depend on the nature of the contribution. For example
     (a) If the contribution is primarily a new algorithm, the paper should make it clear how to reproduce that algorithm.
     (b) If the contribution is primarily a new model architecture, the paper should describe the architecture clearly and fully.
     (c) If the contribution is a new model (e.g., a large language model), then there should either be a way to access this model for reproducing the results or a way to reproduce the model (e.g., with an open-source dataset or instructions for how to construct the dataset).
     (d) We recognize that reproducibility may be tricky in some cases, in which case authors are welcome to describe the particular way they provide for reproducibility. In the case of closed-source models, it may be that access to the model is limited in some way (e.g., to registered users), but it should be possible for other researchers to have some path to reproducing or verifying the results.

5. **Open access to data and code**

Question: Does the paper provide open access to the data and code, with sufficient instructions to faithfully reproduce the main experimental results, as described in supplemental material?

Answer: [Yes]

Justification: All datasets used are publicly available, and we have provided the programming code.

Guidelines:

- The answer NA means that paper does not include experiments requiring code.
- Please see the NeurIPS code and data submission guidelines (`https://nips.cc/public/guides/CodeSubmissionPolicy`) for more details.
- While we encourage the release of code and data, we understand that this might not be possible, so "No" is an acceptable answer. Papers cannot be rejected simply for not including code, unless this is central to the contribution (e.g., for a new open-source benchmark).
- The instructions should contain the exact command and environment needed to run to reproduce the results. See the NeurIPS code and data submission guidelines (`https://nips.cc/public/guides/CodeSubmissionPolicy`) for more details.
- The authors should provide instructions on data access and preparation, including how to access the raw data, preprocessed data, intermediate data, and generated data, etc.
- The authors should provide scripts to reproduce all experimental results for the new proposed method and baselines. If only a subset of experiments are reproducible, they should state which ones are omitted from the script and why.
- At submission time, to preserve anonymity, the authors should release anonymized versions (if applicable).
- Providing as much information as possible in supplemental material (appended to the paper) is recommended, but including URLs to data and code is permitted.

6. **Experimental setting/details**

   Question: Does the paper specify all the training and test details (e.g., data splits, hyperparameters, how they were chosen, type of optimizer, etc.) necessary to understand the results?

   Answer: [Yes]

   Justification: All the settings mentioned in this article are included in the programming.

   Guidelines:

   - The answer NA means that the paper does not include experiments.
   - The experimental setting should be presented in the core of the paper to a level of detail that is necessary to appreciate the results and make sense of them.
   - The full details can be provided either with the code, in appendix, or as supplemental material.

7. **Experiment statistical significance**

   Question: Does the paper report error bars suitably and correctly defined or other appropriate information about the statistical significance of the experiments?

   Answer: [NA]

   Justification: This article concerned the optimization algorithm instead of statistical uncertainties.

   Guidelines:

   - The answer NA means that the paper does not include experiments.
   - The authors should answer "Yes" if the results are accompanied by error bars, confidence intervals, or statistical significance tests, at least for the experiments that support the main claims of the paper.
   - The factors of variability that the error bars are capturing should be clearly stated (for example, train/test split, initialization, random drawing of some parameter, or overall run with given experimental conditions).

- The method for calculating the error bars should be explained (closed form formula, call to a library function, bootstrap, etc.)
- The assumptions made should be given (e.g., Normally distributed errors).
- It should be clear whether the error bar is the standard deviation or the standard error of the mean.
- It is OK to report 1-sigma error bars, but one should state it. The authors should preferably report a 2-sigma error bar than state that they have a 96% CI, if the hypothesis of Normality of errors is not verified.
- For asymmetric distributions, the authors should be careful not to show in tables or figures symmetric error bars that would yield results that are out of range (e.g. negative error rates).
- If error bars are reported in tables or plots, The authors should explain in the text how they were calculated and reference the corresponding figures or tables in the text.

8. **Experiments compute resources**

   Question: For each experiment, does the paper provide sufficient information on the computer resources (type of compute workers, memory, time of execution) needed to reproduce the experiments?

   Answer: [Yes]

   Justification: We have provided the details in Section 7.

   Guidelines:

   - The answer NA means that the paper does not include experiments.
   - The paper should indicate the type of compute workers CPU or GPU, internal cluster, or cloud provider, including relevant memory and storage.
   - The paper should provide the amount of compute required for each of the individual experimental runs as well as estimate the total compute.
   - The paper should disclose whether the full research project required more compute than the experiments reported in the paper (e.g., preliminary or failed experiments that didn't make it into the paper).

9. **Code of ethics**

   Question: Does the research conducted in the paper conform, in every respect, with the NeurIPS Code of Ethics `https://neurips.cc/public/EthicsGuidelines`?

   Answer: [Yes]

   Justification: The research in this article does not involve human subjects and therefore will not be harmful to humans.

   Guidelines:

   - The answer NA means that the authors have not reviewed the NeurIPS Code of Ethics.
   - If the authors answer No, they should explain the special circumstances that require a deviation from the Code of Ethics.
   - The authors should make sure to preserve anonymity (e.g., if there is a special consideration due to laws or regulations in their jurisdiction).

10. **Broader impacts**

    Question: Does the paper discuss both potential positive societal impacts and negative societal impacts of the work performed?

    Answer: [NA]

    Justification: This article is mostly a theoretical and computational work.

    Guidelines:

    - The answer NA means that there is no societal impact of the work performed.
    - If the authors answer NA or No, they should explain why their work has no societal impact or why the paper does not address societal impact.

- Examples of negative societal impacts include potential malicious or unintended uses (e.g., disinformation, generating fake profiles, surveillance), fairness considerations (e.g., deployment of technologies that could make decisions that unfairly impact specific groups), privacy considerations, and security considerations.
- The conference expects that many papers will be foundational research and not tied to particular applications, let alone deployments. However, if there is a direct path to any negative applications, the authors should point it out. For example, it is legitimate to point out that an improvement in the quality of generative models could be used to generate deepfakes for disinformation. On the other hand, it is not needed to point out that a generic algorithm for optimizing neural networks could enable people to train models that generate Deepfakes faster.
- The authors should consider possible harms that could arise when the technology is being used as intended and functioning correctly, harms that could arise when the technology is being used as intended but gives incorrect results, and harms following from (intentional or unintentional) misuse of the technology.
- If there are negative societal impacts, the authors could also discuss possible mitigation strategies (e.g., gated release of models, providing defenses in addition to attacks, mechanisms for monitoring misuse, mechanisms to monitor how a system learns from feedback over time, improving the efficiency and accessibility of ML).

11. **Safeguards**

    Question: Does the paper describe safeguards that have been put in place for responsible release of data or models that have a high risk for misuse (e.g., pretrained language models, image generators, or scraped datasets)?

    Answer: [NA]

    Justification: No such risks are associated with this study.

    Guidelines:

    - The answer NA means that the paper poses no such risks.
    - Released models that have a high risk for misuse or dual-use should be released with necessary safeguards to allow for controlled use of the model, for example by requiring that users adhere to usage guidelines or restrictions to access the model or implementing safety filters.
    - Datasets that have been scraped from the Internet could pose safety risks. The authors should describe how they avoided releasing unsafe images.
    - We recognize that providing effective safeguards is challenging, and many papers do not require this, but we encourage authors to take this into account and make a best faith effort.

12. **Licenses for existing assets**

    Question: Are the creators or original owners of assets (e.g., code, data, models), used in the paper, properly credited and are the license and terms of use explicitly mentioned and properly respected?

    Answer: [Yes]

    Justification: We have cited the original papers that provide the datasets.

    Guidelines:

    - The answer NA means that the paper does not use existing assets.
    - The authors should cite the original paper that produced the code package or dataset.
    - The authors should state which version of the asset is used and, if possible, include a URL.
    - The name of the license (e.g., CC-BY 4.0) should be included for each asset.
    - For scraped data from a particular source (e.g., website), the copyright and terms of service of that source should be provided.
    - If assets are released, the license, copyright information, and terms of use in the package should be provided. For popular datasets, `paperswithcode.com/datasets` has curated licenses for some datasets. Their licensing guide can help determine the license of a dataset.

- For existing datasets that are re-packaged, both the original license and the license of the derived asset (if it has changed) should be provided.
- If this information is not available online, the authors are encouraged to reach out to the asset's creators.

13. **New assets**

    Question: Are new assets introduced in the paper well documented and is the documentation provided alongside the assets?

    Answer: [NA]

    Justification: We do not release new assets.

    Guidelines:

    - The answer NA means that the paper does not release new assets.
    - Researchers should communicate the details of the dataset/code/model as part of their submissions via structured templates. This includes details about training, license, limitations, etc.
    - The paper should discuss whether and how consent was obtained from people whose asset is used.
    - At submission time, remember to anonymize your assets (if applicable). You can either create an anonymized URL or include an anonymized zip file.

14. **Crowdsourcing and research with human subjects**

    Question: For crowdsourcing experiments and research with human subjects, does the paper include the full text of instructions given to participants and screenshots, if applicable, as well as details about compensation (if any)?

    Answer: [NA]

    Justification: This paper does not involve crowdsourcing nor research with human subjects.

    Guidelines:

    - The answer NA means that the paper does not involve crowdsourcing nor research with human subjects.
    - Including this information in the supplemental material is fine, but if the main contribution of the paper involves human subjects, then as much detail as possible should be included in the main paper.
    - According to the NeurIPS Code of Ethics, workers involved in data collection, curation, or other labor should be paid at least the minimum wage in the country of the data collector.

15. **Institutional review board (IRB) approvals or equivalent for research with human subjects**

    Question: Does the paper describe potential risks incurred by study participants, whether such risks were disclosed to the subjects, and whether Institutional Review Board (IRB) approvals (or an equivalent approval/review based on the requirements of your country or institution) were obtained?

    Answer: [NA]

    Justification: This paper does not involve crowdsourcing nor research with human subjects.

    Guidelines:

    - The answer NA means that the paper does not involve crowdsourcing nor research with human subjects.
    - Depending on the country in which research is conducted, IRB approval (or equivalent) may be required for any human subjects research. If you obtained IRB approval, you should clearly state this in the paper.
    - We recognize that the procedures for this may vary significantly between institutions and locations, and we expect authors to adhere to the NeurIPS Code of Ethics and the guidelines for their institution.
    - For initial submissions, do not include any information that would break anonymity (if applicable), such as the institution conducting the review.

16. **Declaration of LLM usage**

Question: Does the paper describe the usage of LLMs if it is an important, original, or non-standard component of the core methods in this research? Note that if the LLM is used only for writing, editing, or formatting purposes and does not impact the core methodology, scientific rigorousness, or originality of the research, declaration is not required.

Answer: [NA]

Justification: The core contributions of this research are independent of LLMs.

Guidelines:

- The answer NA means that the core method development in this research does not involve LLMs as any important, original, or non-standard components.
- Please refer to our LLM policy (`https://neurips.cc/Conferences/2025/LLM`) for what should or should not be described.